JOURNAL OF MATERIALS SCIENCE 31 (1996) 2081–2089

Linear and non-linear conductive spectra of polyethylene oxide/salt complex

Y. TAJITSU
Science and Engineering Research Laboratory, Waseda University, 1136 Okuboyama, Nishitomita, Honjyo-shi, Saitama 367, Japan

A new experimental system has been developed, which enables measurements of linear as well as non-linear complex conductivities to be made. The frequency dependence of linear to fifth-order non-linear complex conductivities at different temperatures in a polyethylene oxide/salt complex can then be measured. A characteristic conduction relaxation phenomenon was observed in the spectra, which suggested the existence of different ion-conduction mechanisms between the high- and low-frequency regions. It was also found that the ratio of linear to non-linear conductivities was closely related to the elementary process of ionic transport. Furthermore, this ratio obtained from non-linear measurements allowed an estimate of the important parameters which characterized ionic transport in ion-conducting polymers, such as the hopping distance of an ion or the size of a connected cluster of the site capable of ion hopping, without the need for any additional assumptions. Thus, it was found that in a polyethylene oxide/salt complex, the typical size of a connected cluster of the effective sites capable of ion hopping was approximately 4 nm.

1. Introduction

In the past, studies on ion-conducting polymers have centred around polyethylene oxide and alkali metal salt complexes [1–6]. These studies were initiated by the series of studies conducted by Wright and co-workers in the 1970s, who found relatively high conductivity in the polyethylene oxide/salt complex [1–3]. Studies in this field were further promoted by the report of Armand [7] who indicated that the complex of polyethylene oxide and alkali metal salt, in particular lithium salt, was a lithium-ion conductive solid electrolyte, and that it could possibly be applied to solid-state batteries, for example. Various new ion-conducting polymers have been produced with the aim of actual utilization [1–7].

Polymers adsorbing low molecular weight compounds such as water have been known to show high ionic conductivity. In such polymers, the direct cause of high ionic conductivity, for example, dissociation and transfer of ions, depends on the type of low molecular weight compounds, and polymers themselves basically play the role of a matrix. In contrast, ion-conducting polymers are solids with high concentrations of dissolved electrolytes [4, 5]. Therefore, the polymers themselves induce higher ionic conductivity than that of typical ionic solids such as NaCl [4, 5]. Clarification of the mechanism behind polymer and ion interaction is one of the issues that has been attracting the attention of many researchers in various fields [1–7].

The temperature dependence of d.c. conductivity, $\sigma_{d.c.}$, in ion-conducting polymers [4, 5] is generally of the following Williams–Landel–Ferry (WLF) type [8]

$$\log\frac{\sigma_{d.c.}(T)}{\sigma_{d.c.}(T_g)} = \frac{C_1(T-T_g)}{C_2+(T-T_g)} \quad (1)$$

or Vogel–Tamman–Fulcher (VTF) type [9–11]

$$\sigma_{d.c.}(T) = \frac{A_1}{T^{1/2}}\frac{-A_2}{e^{T-T_0}} \quad (2)$$

where C_1, C_2, A_1 and A_2 are constants. T_g is the glass transition temperature, and T_0 is the temperature at which configuration entropy becomes zero. To explain this temperature dependence of the d.c. conductivity, the free-volume model [12] and its expansion, the configuration entropy model [13, 14], are often used. Assuming the cooperative nature of ionic transfer and local motion of polymer chains, the temperature dependence of mobility is calculated on the basis of local motion of polymer chains, and the temperature dependence of conductivity is presented based on this explanation [4–6, 14].

Detailed information regarding the correlation between ionic transport and dynamic behaviour of the polymer chain is expected to be obtained from the investigation of the frequency dependence of conductivity. In order to obtain useful information on this correlation, the frequency dependence of permittivity and conductivity in ion-conducting polymers was measured by many researchers [4, 5, 15–19]. However, although the above-mentioned free-volume model is effective in explaining d.c. conductivity because thermodynamics is introduced for the explanation of

0022–2461

static states, it is useless in explaining the frequency dependence of conductivity.

As a model to explain the frequency dependence of conductivity in ion-conducting polymers, the dynamic percolation model, an expansion of the percolation model, was proposed by Ratner *et al.* [20] and Harison and Zwanzig [21]. However, the dynamic percolation model is very complex, because it contains many physical constants in equations representing the frequency dependence of conductivity which cannot be determined experimentally. Therefore, in order to explain the frequency dependence of conductivity obtained by experiments, many assumptions must be made for the physical constants. Thus, although this model is theoretically established, complete verification of its validity by experiments is actually difficult to accomplish.

It has been noted that studies on non-linear spectra of conductivity may provide information regarding the elementary processes of ionic transport and formation of potential energy, which is difficult to obtain from measurements in the linear region. With respect to non-linearity of permittivity, pioneers Furukawa *et al.* [22] studied ferroelectric polymers. Referring to the methods used in their study, we have further advanced this field of research to develop a measurement system for non-linear conductive spectra. In this study, the newly developed measurement system was used to measure the temperature dependence of linear to fifth-order non-linear complex conductive spectra in a polyethylene oxide/salt complex. The observed non-linear conductive spectrum exhibited a very complicated form including a relaxation phenomenon. By detailed analysis of these non-linear spectra, various parameters, such as non-linear d.c. conductivities and non-linear relaxation strength, were evaluated. Furthermore, the conduction mechanism of ions was studied using these evaluated parameters in an analytical method which took advantage of the characteristics of experiments on non-linear conductivity.

2. Experimental procedure

When the direct current, $I_{\mathrm{d.c.}}$, for a non-linear system is expanded in odd powers of the static electric field, E

$$I_{\mathrm{d.c.}} = \sigma_{1\,\mathrm{d.c.}}E + \sigma_{3\,\mathrm{d.c.}}E^3 + \sigma_{5\,\mathrm{d.c.}}E^5 + \cdots \quad (3)$$

we can express the linear and non-linear conductivities in terms of coefficients of the exponents. Here $\sigma_{1\,\mathrm{d.c.}}$ is the linear d.c. conductivity. The coefficient $\sigma_{n\,\mathrm{d.c.}}$ for $n \geqslant 3$ defines the nth-order non-linear d.c. conductivity. However, when excitation is not a static field but a sinusoidal electric field, it is complicated in that complex non-linear conductivity is defined. On the other hand, complex non-linear permittivities have been already reported by Furukawa *et al.* [22].

For measurements of linear and non-linear conductivities, we applied a sinusoidal electric field

$$E(t) = E_0 \cos \omega t \quad (4)$$

with amplitude, E_0, and angular frequency, ω. If there exists a relaxation phenomenon in a sample, the response of electric current, $I(t)$, is represented by

$$I(t) = \sum_{n=1}^{\infty} (I'_n \cos n\omega t + I''_n \sin n\omega t) \quad (5)$$

We have detected the in-phase and 90° out-of-phase components of the electric current, $I(t)$, with frequency $n\omega$. The phenomenological theory of stationary linear response is well established on the basis of Boltzmann's superposition principle. On the other hand, extending this theory of stationary linear response to a non-linear system, Nakada has developed a phenomenological theory of the non-linear relaxation response [23]. According to this theory, the resulting response can be expressed by a sum of convolution integrals of the applied electric field at multiple time points and the non-linear after-effect functions. When the excitation is given by Equation 4, the resulting response, $I(t)$, is calculated as follows

$$\begin{aligned} I(t) = {} & [\sigma'_1(\omega)\cos \omega t + \sigma''_1(\omega)\sin \omega t]E_0 + \\ & [\sigma'_3(3\omega)\cos 3\omega t + \sigma''_3(3\omega)\sin 3\omega t + \\ & B'_3(\omega)\cos \omega t + B''_3(\omega)\sin \omega t]E_0^3 + \\ & [\sigma'_5(5\omega)\cos 5\omega t + \sigma''_5(5\omega)\sin 5\omega t + \cdots] \\ & E_0^5 + \cdots \end{aligned} \quad (6)$$

where $\sigma'_1(\omega)$ and $\sigma''_1(\omega)$ are the real and imaginary parts of linear complex conductivity $\sigma^*_1(\omega) = \sigma'_1(\omega) + j\sigma''_1(\omega)$, respectively. $\sigma'_n(n\omega)$ and $\sigma''_n(n\omega)$ are also the real and imaginary parts of nth-order ($n = 3, 5, \ldots$) non-linear complex conductivities $\sigma^*_n(n\omega) = \sigma'_n(n\omega) + j\sigma''_n(n\omega)$, respectively.

Comparing Equations 6 and 5, we find relationships between the amplitude of the in-phase component, I'_n, and the amplitude of the applied field, E_0, as follows

$$I'_1 = \sigma'_1(\omega)E_0 + \frac{3}{4}\sigma'_3(\omega)E_0^3 + \cdots \quad (7)$$

$$I'_3 = \frac{1}{4}\sigma'_3(3\omega)E_0^3 + \frac{5}{16}\sigma'_3(3\omega)E_0^5 + \cdots \quad (8)$$

$$I'_5 = \frac{1}{16}\sigma'_5(5\omega)E_0^5 + \cdots \quad (9)$$

Furthermore, the relationships between 90° out-of-phase components, $I''_n (n = 1, 3, 5, \ldots)$, and E_0 are of the same forms as those of Equations 7–9, respectively

$$I''_1 = \sigma''_1(\omega)E_0 + \frac{3}{4}\sigma''_3(\omega)E_0^5 + \cdots \quad (10)$$

$$I''_3 = \frac{1}{4}\sigma''_3(3\omega)E_0^3 + \frac{5}{16}\sigma''_3(3\omega)E_0^5 + \cdots \quad (11)$$

$$I''_5 = \frac{1}{16}\sigma''_5(5\omega)E_0^5 + \cdots \quad (12)$$

As a result, we have determined the real component, $\sigma'_n(n\omega)$, and the imaginary component, $\sigma''_n(n\omega)$, of linear and non-linear complex conductivities,

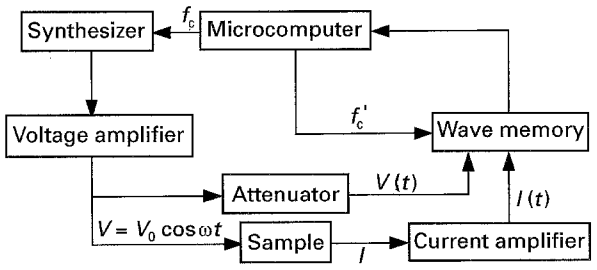

Figure 1 Schematic diagram of an experimental system for non-linear complex conductivity measurements.

$\sigma_n^*(n\omega) = \sigma_n'(n\omega) + j\sigma_n''(n\omega)$, as follows

$$\sigma_n'(n\omega) = \frac{2^{n-1} I_n'}{E_0^n} \quad (13a)$$

$$\sigma_n''(n\omega) = \frac{2^{n-1} I_n''}{E_0^n} \ (n = 1, 3, 5, \cdots) \quad (13b)$$

Owing to their complexity, the terms $\sigma_n^*(n\omega)$, $\sigma_n'(n\omega)$ and $\sigma_n''(n\omega)$ are abbreviated below to σ_n^*, σ_n', σ_n'', respectively. The complex permittivities, $\varepsilon_n^*(n\omega) = \varepsilon_n'(n\omega) - j\varepsilon_n''(n\omega)$, can be calculated from $\sigma_n^* = \sigma_n' + j\sigma_n''$ as

$$\sigma_n' = n\omega\varepsilon_n''(n\omega) \quad (14a)$$

$$\sigma_n'' = n\omega\varepsilon_n'(n\omega) \quad (14b)$$

The terms $\varepsilon_n^*(n\omega)$, $\varepsilon_n'(n\omega)$ and $\varepsilon_n''(n\omega)$ are abbreviated to ε_n^*, ε_n', ε_n''.

Based on this principle, we have developed a new experimental system which enables measurements of linear as well as non-linear complex conductivities $\sigma_n^* = \sigma_n' + j\sigma_n''$ $(n = 1, 3, 5)$ in the frequency range of 25 mHz to 5 MHz. Fig. 1 shows a schematic diagram of the experimental system. The excitation wave is propagated to a sample. The induced current of the electrode is detected by a current amplifier. The fundamental and higher harmonic responses are then measured according to Equation 5, and the voltage and current signals are simultaneously stored in a wave memory. The detected data can also be calculated in a microcomputer.

Using this system, we examined a variety of ion-conducting polymers including polyethylene oxide and its derivatives [24, 25]. Special attention was paid to a polyethylene oxide (PEO) whose characteristics were improved by the addition of SiO_2 [24] and doping with $LiClO_4$ (Li^+/EOunit = 0.1). We believe that the polyethylene oxide modified by SiO_2 addition and doping with $LiClO_4$ exhibits lower crystallinity than other unmodified systems on the basis of its X-ray diffraction pattern [24]. The glass transition point, T_g, was determined to be about $-30\,^\circ C$ by dynamical mechanical measurements.

Typical experimental results of the electric field dependence of the in-phase component I_n' $(n = 1, 3, 5)$ in the electric current are shown in Fig. 2. In the top figure, I_1' is plotted against the amplitude, E_0, of the electric field. Using Equation 7, we have obtained σ_1' from the gradient of the linear relationship. When I_3' is plotted against the third power of E_0, we obtain

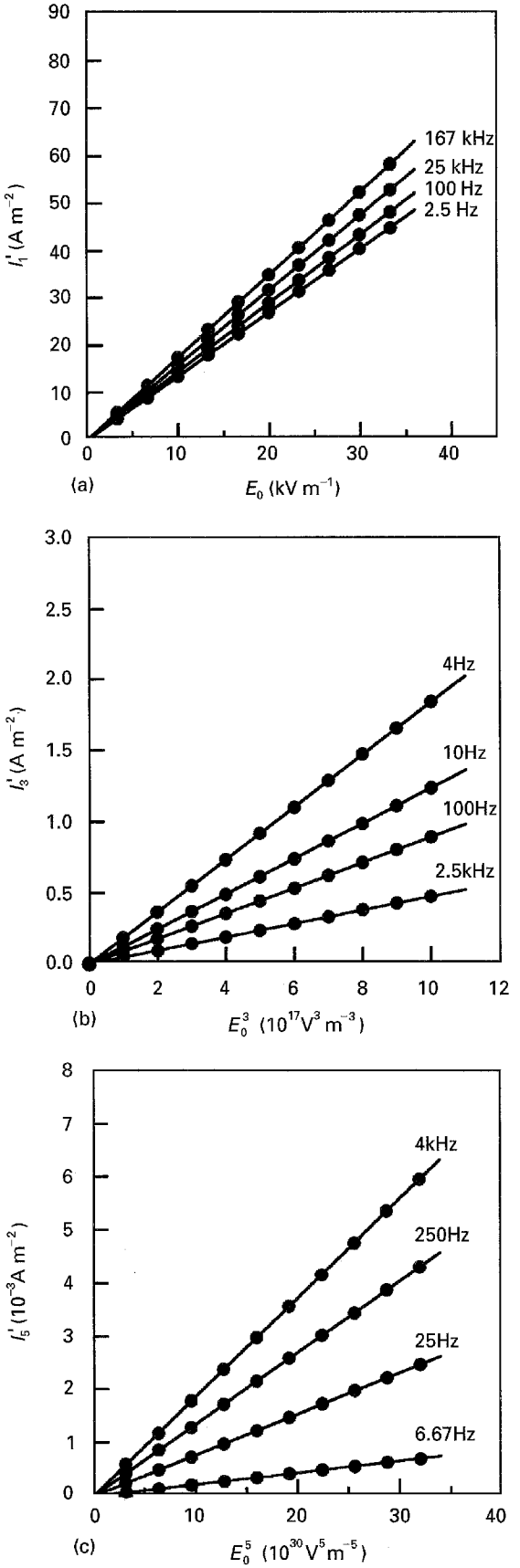

Figure 2 Dependence of the in-phase components of the (a) linear, (b) third-order and (c) fifth-order harmonic electric currents, I_1', I_3' and I_5', as a function of the amplitude of applied field E_0.

σ_3' from the slope referring to Equation 8. In the bottom figure, I_5' is plotted against the fifth power of E_0. We also obtain σ_5' from the slope. Using the same method, we can obtain the imaginary part σ_n'' of the complex linear and non-linear conductivities.

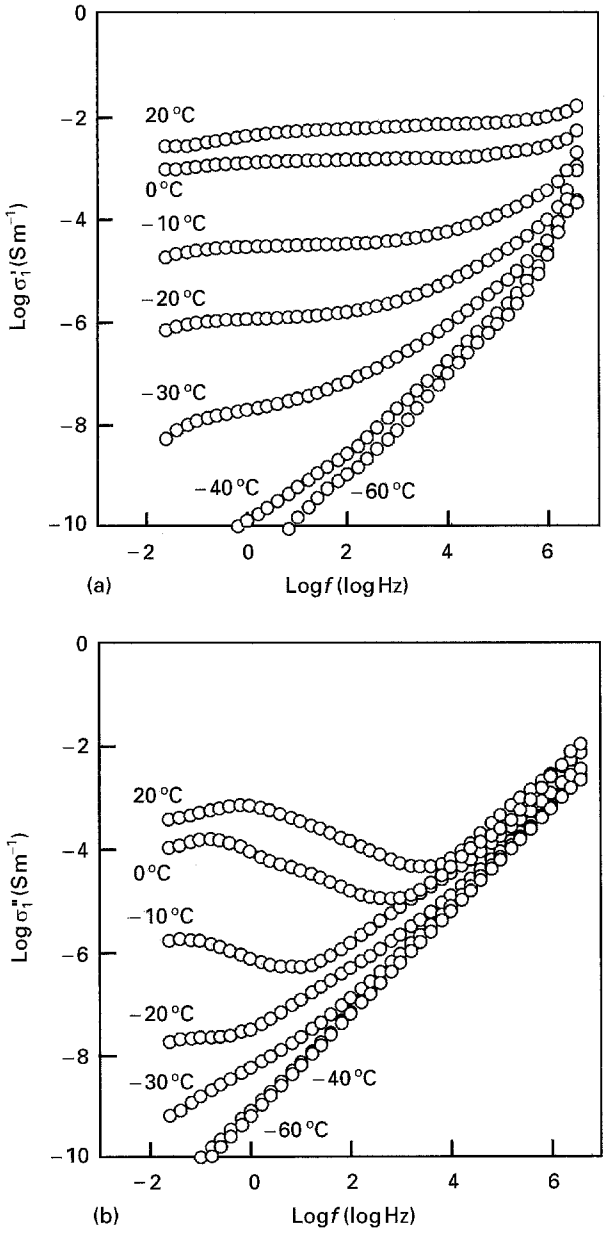

Figure 3 Frequency spectra of the (a) real and (b) imaginary components of the linear conductivity.

3. Results

Fig. 3 shows the frequency spectra of the linear conductivity $\sigma_1^* = \sigma_1' + j\sigma_1''$. At 20 °C, σ_1' remains nearly constant in the low-frequency range and σ_1'' shows a peak. Both σ_1' and σ_1'' increase with increasing frequency. With decreasing temperature, the spectra shift to the lower frequency region. Results of the third-order non-linear conductivity $\sigma_3^* = \sigma_3' + j\sigma_3''$ and the fifth-order non-linear conductivity $\sigma_5^* = \sigma_5' + j\sigma_5''$ are shown in Figs 4 and 5, respectively. It is found that σ_3^* and σ_5^* show characteristic frequency spectra consisting of the peaks of σ_3'' and σ_5'', respectively. As temperature is decreased, the spectra shift to the lower frequency region with a considerable reduction of peak height.

An attempt was made to reproduce the observed linear conductive spectra using the total conductivity σ_{1b}^*

$$\sigma_{1b}^* = \sigma_{1d.c.} + \sigma_{1relax}^* + j\omega(\varepsilon_{1in} - j\varepsilon_{1loss}) \quad (15)$$

$$\sigma_{1relax}^* = \Delta\sigma_1 \frac{(j\omega\tau_1)^{\alpha_1\beta_1}}{[1 + (j\omega\tau_1)^{\beta_1}]^{\alpha_1}} \quad (16)$$

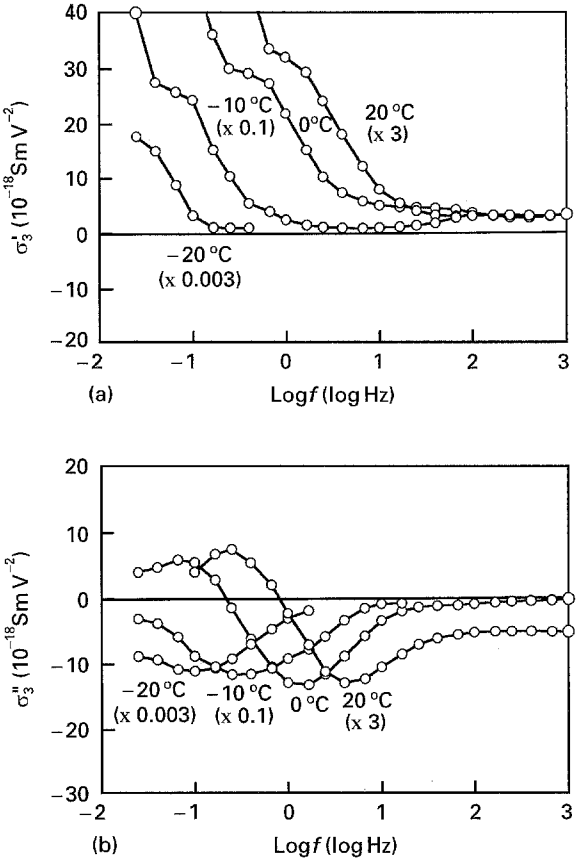

Figure 4 (a, b) Frequency spectra of the third-order non-linear conductivity.

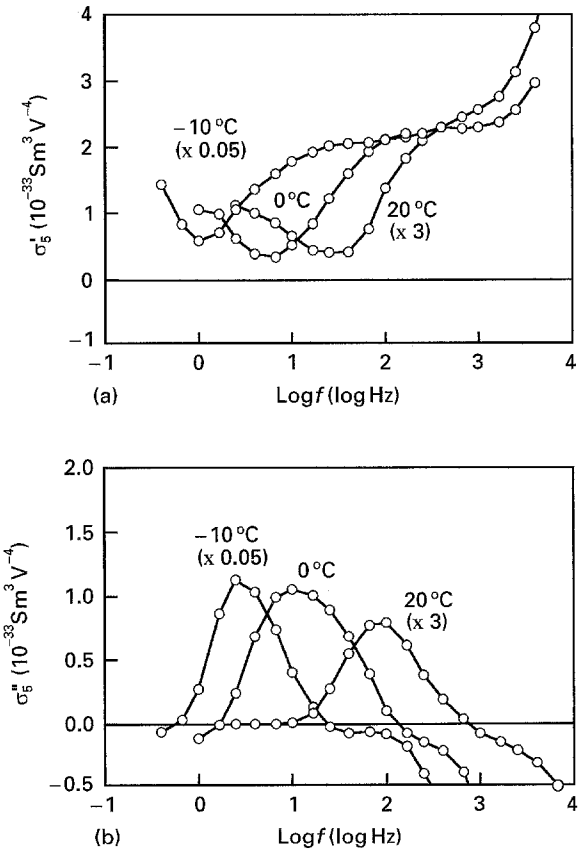

Figure 5 (a, b) Frequency spectra of the fifth-order non-linear conductivity.

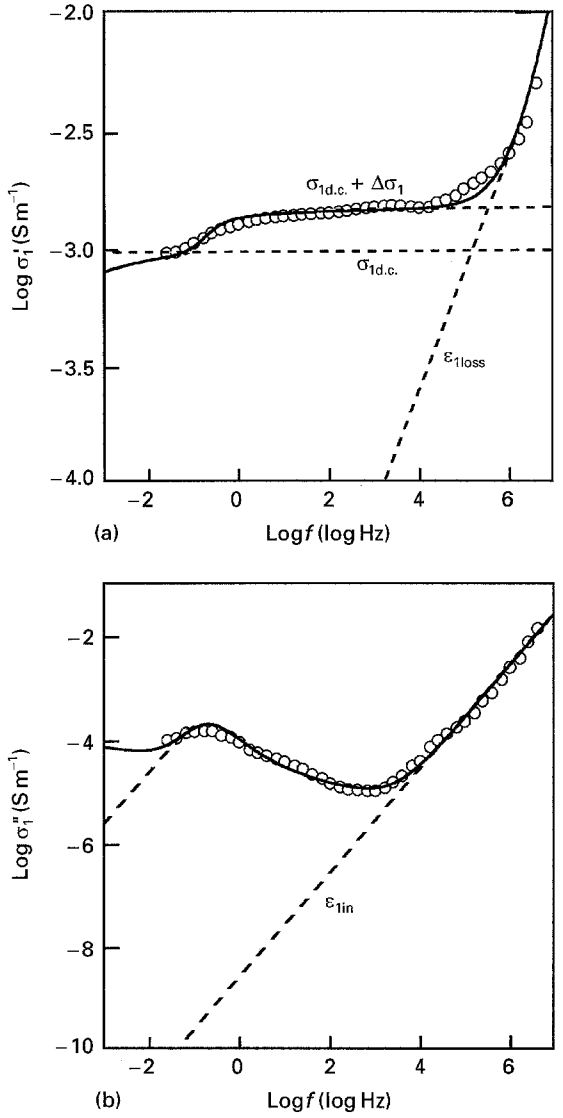

Figure 6 (a, b) Comparison of (○) observed and (—) fitted frequency spectra of the linear conductivity at 0 °C.

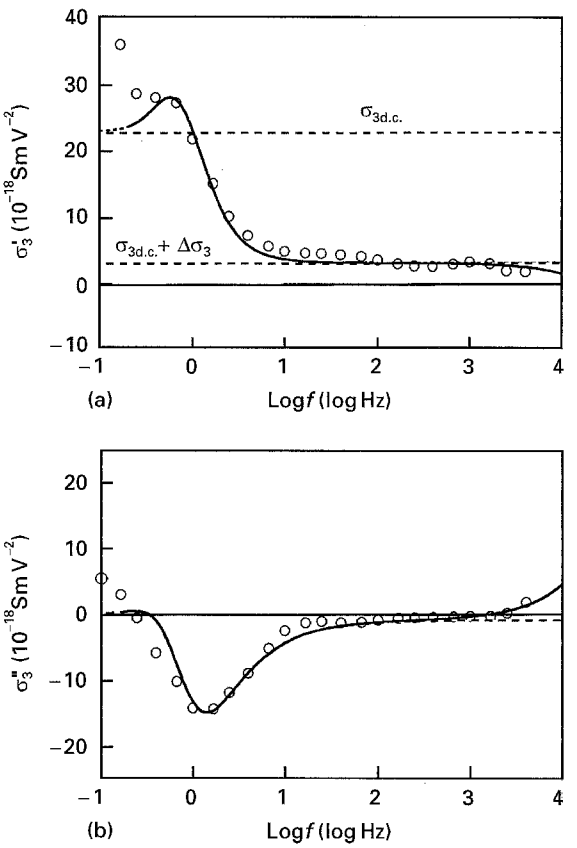

Figure 7 (a, b) Comparison of (○) observed and (—) fitted frequency spectra of the third-order non-linear conductivity at 0 °C.

where $\sigma_{d.c.}$ is the d.c. conductivity, $\Delta\sigma_1$ is the relaxation strength, and τ_1 is the relaxation time. β_1 is a parameter expressing the distribution of relaxation times. α_1 describes the skewness of the dispersion. $\varepsilon_{1\,in}$ and $\varepsilon_{1\,loss}$ in Equation 15 are the real and imaginary parts, respectively, of the permittivity which is assumed to be independent of frequency. The effect of electrode polarization can be expressed by an equivalent capacitance, ε^*_{el} [26]

$$\varepsilon^*_{el} = \varepsilon_{elo}(j\omega)^{m-1}\,(m < 1) \tag{17}$$

which is connected in series with σ^*_{1b}. Thus the linear complex conductivity $\sigma^*_1 = \sigma'_1 + j\sigma''_1$ of the sample is given by

$$\sigma^*_1 = \left(\frac{1}{\sigma^*_{1b}} + \frac{1}{j\omega\varepsilon^*_{el}}\right)^{-1} \tag{18}$$

Using the least squares method, we determine the constants, for example, $\sigma_{1\,d.c.}$ and $\Delta\sigma_1$, in Equations 15–17. Fig. 6 shows a typical example of the results. In both σ'_1 and σ''_1 of linear complex conductivity, σ^*_1, the experimental data (○) obtained at 0 °C, are shown to be reasonably well reproduced by Equation 18. In the low-frequency region below 0.1 Hz, the difference in tendency between the solid line and the dashed line corresponding to d.c. conductivity, $\sigma_{1\,d.c.}$, indicates the effect of electrode polarization. Applying this analytical method to experimental results obtained at various temperatures, it is found that the electrode polarization does not affect the observed spectra in the frequency region higher than 1 Hz.

We next attempted to reproduce the observed non-linear conductive spectra. We assumed the equation

$$\sigma^*_n = n\sigma_{nd.c.} + n\sigma^*_{nrelax} + jn\omega(\varepsilon_{nin} - j\varepsilon_{nloss}) \tag{19}$$

$$\sigma^*_{nrelax} = \Delta\sigma_n \frac{(j\omega\tau_n)^{n\alpha_n\beta_n}}{[1 + (j\omega\tau_n)^{\beta_n}]^{n\alpha_n}} \tag{20}$$

with $n = 3, 5$ where the suffix n represents the nth-order non-linear conductivities. Here $\sigma_{n\,d.c.}$ is the nth-order d.c. conductivity, $\Delta\sigma_n$ is the relaxation strength and τ_n is the relaxation time. β_n is a parameter expressing the distribution of relaxation times and α_n describes the skewness of the dispersion. $\varepsilon_{n\,in}$ and $\varepsilon_{n\,loss}$ in Equation 19 are the real and imaginary parts, respectively, of the permittivity which is assumed to be independent of frequency. Fig. 7 shows an example of the results of the third-order complex non-linear conductivity $\sigma^*_3 = \sigma'_3 + j\sigma''_3$ at 0 °C. The experimental data are shown to be reasonably well reproduced by Equation 19 with $n = 3$. Fig. 8 shows a typical example of results of the fifth-order complex non-linear conductivity $\sigma^*_5 = \sigma'_5 + j\sigma''_5$ at 0 °C. Good agreement between the observed data and those calculated by Equation 19 with $n = 5$, has been obtained.

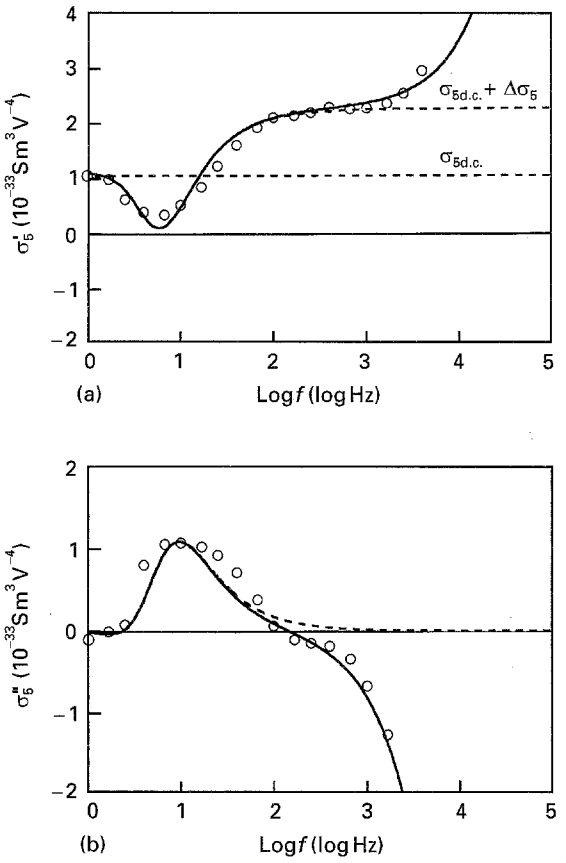

Figure 8 (a, b) Comparison of (○) observed and (—) fitted frequency spectra of the fifth-order non-linear conductivity at 0 °C.

From Figs 6–8, we found that the solid curves calculated from Equation 19 reproduce the respective observed spectra reasonably well. The typical results of these best-fit parameters obtained by the same method are summarized in Table I.

The function of the linear conductive relaxation, $\sigma^*_{1\,\mathrm{relax}}$, in Equation 15 results in a decrease in conductivity from $\sigma_{1\,\mathrm{d.c.}} + \Delta\sigma_1$ to $\sigma_{1\,\mathrm{d.c.}}$ with decreasing frequency. Equation 15 is of the same form as that of Equation 19 with $n = 1$. When α_1, β_1 and n equal one, the relaxation part in Equation 19 is essentially the same as the linear dielectric relaxation function [27]. The corresponding dielectric relaxation strength over 100 suggests that the ionic motions accompany a large dielectric polarization. On the basis of these results, we speculate that there are two separate conduction mechanisms in a polyethylene oxide/salt complex. The high-frequency conduction could be attributed to the rather free motion of ions which hop to adjacent sites to yield a conductivity of $\sigma_{1\,\mathrm{d.c.}} + \Delta\sigma_1$. Such motion seems to occur in limited domains. At low frequencies, ions reach the edge of such domains to generate polarization and yield a low conductivity, $\sigma_{1\,\mathrm{d.c.}}$, governed by their hopping to adjacent domains. Upon further development of these speculations, we reach much the same conclusion with regard to ion transport as the dynamic percolation theory [20, 21].

Furthermore, an explanation for non-linear conductivities is necessary. The non-linear dielectric relaxation function, $\varepsilon^*_{n\,\mathrm{relax}}$ [22, 23]

$$\sigma^*_{n\mathrm{relax}} = jn\omega\varepsilon^*_{n\mathrm{relax}} \tag{21}$$

$$\varepsilon^*_{n\mathrm{relax}} = \frac{\Delta\varepsilon_n}{[1 + (j\omega\tau_n)^{\beta_n}]^{n\alpha_n}} \tag{22}$$

with $n = 3, 5$ does not affect the non-linear conductivity at either low or high frequencies. We have already found that the non-linear relaxation part, $\sigma^*_{n\,\mathrm{relax}}$, with $n = 3$ or 5 in Equation 19 is not the same as the non-linear dielectric relaxation function, $\varepsilon^*_{n\,\mathrm{relax}}$ in Equation 21, even if $\alpha_n = \beta_n = 1$. In other words, the non-linear relaxation, $\sigma^*_{n\,\mathrm{relax}}$ in Equation 19 affects the non-linear conductivity at both low and high frequencies. This effect in Equation 19 is worth noting.

4. Discussion

The ion-conducting property of the system has been already determined on the basis of the fundamental principle with regard to ion transport in each model [4–6]. Moreover, the basic parameters of each model, such as the distance of ion hopping between available sites, are related to this fundamental principle. On the basis of these factors, the conduction mechanism of ions in ion-conducting polymers is studied using an analytical method which takes advantage of the characteristics of experiments on non-linear conductivity. Now, we show two typical examples of results from the application of this analytical method using non-linear measurements to the models of ion transport in a polyethylene oxide/salt complex developed by many theorists [4–6]. One involves the dynamic percolation model [4, 6] and the other the hopping and variable-range hopping model [28].

The dynamic percolation model characterizes ionic motion in terms of hopping between neighbouring positions [4, 6, 20, 21]. This model developed by Ratner *et al.* [20] takes into account the dependence of ionic motion rates on the fluidity, or rate of segmental motion, of polymer host. A characteristic rate of

TABLE I The d.c. conductivity and conductive relaxation strength obtained as best-fit parameters at various temperatures

	d.c. conductivity			Conductive relaxation strength		
T (°C)	$\sigma_{1\mathrm{d.c.}}$ (Sm^{-1})	$\sigma_{3\mathrm{d.c.}}$ (Sm V^{-2})	$\sigma_{5\mathrm{d.c.}}$ (Sm^3 V^{-4})	$\Delta\sigma_1$ (Sm^{-1})	$\lvert\Delta\sigma_3\rvert$ (Sm V^{-2})	$\Delta\sigma_5$ (Sm^3 V^{-4})
−10	2.38×10^{-5}	2.51×10^{-18}	9.51×10^{-35}	9.12×10^{-6}	2.40×10^{-18}	1.52×10^{-35}
0	9.80×10^{-4}	2.28×10^{-17}	1.05×10^{-33}	5.24×10^{-4}	1.98×10^{-17}	1.23×10^{-33}
10	1.98×10^{-3}	5.62×10^{-17}	1.99×10^{-33}	2.02×10^{-3}	5.01×10^{-17}	2.51×10^{-33}
20	2.95×10^{-3}	9.05×10^{-17}	3.03×10^{-33}	4.05×10^{-3}	8.01×10^{-17}	4.51×10^{-33}

renewal, λ, is defined, which characterizes the rate at which a motion pathway from one site to another becomes available for ion motion. That is to say, the motion of the ion is controlled by the dynamics of the polymer host and cannot occur unless it is promoted by segmental motion of the polymer host [4, 6, 20]. This leads to typical curved Arrhenius plots for conductivity, and a suggestion that decreasing the glass transition temperature as much as possible yields maximal ionic mobility [4, 6]. The characteristic of the dynamic percolation model is that the ion transport on a percolation lattice both above and below threshold f_c can be understood using the same general formalism, including frequency and temperature dependence [4–6, 20].

We first apply the dynamic percolation model [20] to the observed conductive spectra. Following the dynamic percolation model, the resulting conductivity, $\sigma(\omega)$, at frequency ω may be given by

$$\sigma(\omega) = \frac{n_e e^2}{kT} \int_0^\infty e^{-j\omega t} \sum_s s^2 e^{-\lambda t} p_0(s, t) \mathrm{d}t \quad (23)$$

where n_e is the carrier density, T the absolute temperature, k the Boltzmann constant, e the elementary charge, and $p_0(s, t)$ the conditional probability on site s at time t. The exact solution of the integration shown above as obtained by Druger *et al.* [20] is very complicated; thus it is difficult to analyse the observed spectra of linear and non-linear conductivities using their solution. We therefore have to obtain an approximate solution to describe the behaviour of the conductivities in the dynamic percolation model. We can find approximate solutions for both the small ω and large ω behaviour for $\sigma(\omega)$ by expanding Equation 23, as follows

$$\sigma_{\mathrm{d.c.}\,(\omega=0)} = \frac{n_d n_e \lambda \alpha e^2 \langle r^2 \rangle_0}{(\lambda + \alpha) kT} \quad (24)$$

and

$$\sigma_{\mathrm{h}\,(\omega=\infty)} = \frac{n_d n_e \alpha e^2 \langle r^2 \rangle_0}{kT} \quad (25)$$

with

$$\alpha = \alpha_0 n_s f(s) W \quad (26)$$

where $\langle r^2 \rangle_0$ is the mean-squared displacement on the static percolation lattice as t approaches infinity, α_0 is the transformation coefficient, n_s is the probability of existence on site s, n_d is the dimensional constant, $f(s)$ is the fraction of bonds on site s and W is the mean hopping rate between available sites.

Now we are ready to calculate direct current, $I_{\mathrm{d.c.}}$, and current, I_h, at high frequency on the basis of Equations 24 and 25, respectively. When $I_{\mathrm{d.c.}}$ and I_h are expanded in odd powers of E, we can express the linear and non-linear conductivities in terms of coefficients of exponents as follows

$$I_{\mathrm{d.c.}} = \sigma_{1\mathrm{d.c.}} E + \sigma_{3\mathrm{d.c.}} E^3 + \sigma_{5\mathrm{d.c.}} E^5 + \cdots \quad (\lambda < \alpha) \quad (27)$$

$$\sigma_{1\mathrm{d.c.}} = \frac{n_d n_e e^2 \langle r^2 \rangle_0}{kT} \left[\lambda - \frac{\lambda^2 kT \exp(\Delta U/kT)}{\alpha_0 f(s) n_s e a^*} \right] \quad (28)$$

$$\sigma_{3\mathrm{d.c.}} = \frac{\lambda^2 e n_d n_e \langle r^2 \rangle_0 \exp(\Delta U/kT)}{3\alpha_0 f(s) n_s a} \left(\frac{ea^*}{2KT} \right)^3 \quad (29)$$

$$\sigma_{5\mathrm{d.c.}} = \frac{3\lambda^2 e n_d n_e \langle r^2 \rangle_0 \exp(\Delta U/kT)}{1420\alpha_0 f(s) n_s a^*} \left(\frac{ea^*}{2KT} \right)^5 \quad (30)$$

$$I_h = \sigma_{1h} E + \sigma_{3h} E^3 + \sigma_{5h} E^5 + \cdots \quad (31)$$

$$\sigma_{1h} = \frac{2 n_d n_e n_s \alpha_0 f(s) e^2 \langle r^2 \rangle_0 \exp(-\Delta U/kT)}{kT} \left(\frac{ea^*}{2KT} \right) \quad (32)$$

$$\sigma_{3h} = \frac{n_d n_e n_s \alpha_0 f(s) e^2 \langle r^2 \rangle_0 \exp(-\Delta U/kT)}{3kT} \left(\frac{ea^*}{2KT} \right)^3 \quad (33)$$

$$\sigma_{5h} = \frac{n_d n_e n_s \alpha_0 f(s) e^2 \langle r^2 \rangle_0 \exp(-\Delta U/kT)}{60kT} \left(\frac{ea^*}{2KT} \right)^5 \quad (34)$$

where $\sigma_{n\mathrm{d.c.}}$ is the nth-order d.c. conductivity and σ_{nh} is nth-order conductivity at high frequency. ΔU is the activation energy and a^* is the typical size of a connected cluster of the effective sites capable of ion hopping per characteristic time. Because Equations 3 and 27 turn out to be exactly the same, we can obtain expressions for linear and non-linear d.c. conductivities, $\sigma_{n\mathrm{d.c.}}$, using the dynamic percolation model. We also obtain linear and non-linear conductivities, σ_{nh}, at high frequency from Equation 31. The obtained expressions for $\sigma_{n\mathrm{d.c.}}$ and σ_{nh} contain many physical quantities which cannot be obtained experimentally. However, the cluster size, a^*, can be obtained experimentally by our method, as described below. If we take the ratios of $\sigma_{n\mathrm{d.c.}}$ to $\sigma_{m\mathrm{d.c.}}$ and σ_{nh} to σ_{mh} (n and $m = 1, 3, 5$), we find simple equations as follows

$$\frac{\sigma_{5\mathrm{d.c.}}}{\sigma_{3\mathrm{d.c.}}} = \frac{9e^2 a^{*2}}{5680 k^2 T^2} \quad (35)$$

$$\frac{\sigma_{3h}}{\sigma_{1h}} = \frac{e^2 a^{*2}}{24 k^2 T^2} \quad (36)$$

$$\frac{\sigma_{5h}}{\sigma_{3h}} = \frac{e^2 a^{*2}}{80 k^2 T^2} \quad (37)$$

On the other hand, the ratio $\sigma_{3\mathrm{d.c.}}/\sigma_{1\mathrm{d.c.}}$ is omitted from the above list, because many physical quantities, which cannot be obtained experimentally, remain. Equations 35–37 contain only measurable parameters. Substituting three parameters, e, k and T into Equations 35–37, a^* is obtained without any additional assumptions. The case of interest here is that a^* calculated by Equations 35–37 should equal each other. We substitute $\sigma_{3\mathrm{d.c.}}$ and $\sigma_{5\mathrm{d.c.}}$, obtained as best-fit parameters in linear and non-linear conductive spectra at each temperature, into Equation 35. As a result, we obtain $a^* \simeq 5$ nm, nearly independent of temperature. In much the same way, we also obtain

$a^* \simeq 4$ nm, substituting σ_{1h}, σ_{3h} and σ_{5h} into Equations 36 and 37. It is of importance that the two estimates approximate each other well, because a^* calculated by Equations 35–37 should be equal, as mentioned above. This finding supports the appropriateness of our method; that is, a^* is obtained exactly using this method. We consider next the physical meaning of a^*. Below the static percolation threshold, the carrier is typically limited to a region of characteristic dimensions within each renewal interval in the dynamic percolation model. Consequently, it is sufficient to understand that the obtained a^* of 4–5 nm corresponds to the typical size of a connected cluster of available sites capable of ion hopping. Therefore, $a^* \simeq 4$–5 nm in the dynamic percolation model is suitable in terms of elucidation of the mechanism of ion transport in a polyethylene oxide/salt complex, even when its structure has been taken into consideration [4–6, 24].

Keeping the above-mentioned conclusion in mind, we consider next the case where our non-linear method is applied to another model. Using the hopping and variable-range hopping model [28] in which the ion is transferred by hopping between sites, the resulting direct current, $I_{d.c.}$, is given by

$$I_{d.c.} = \sigma_{1d.c.} E + \sigma_{3d.c.} E^3 + \sigma_{5d.c.} E^5 + \cdots \quad (38)$$

$$\sigma_{1d.c.} = \frac{e^2 a^2 P_0 N}{kT} \exp\left(-\frac{\Delta U}{kT}\right) \quad (39)$$

$$\sigma_{3d.c.} = \frac{e^4 a^4 P_0 N}{24 k^3 T^3} \exp\left(-\frac{\Delta U}{kT}\right) \quad (40)$$

$$\sigma_{5d.c.} = \frac{e^6 a^6 P_0 N}{1920 k^5 T^5} \exp\left(-\frac{\Delta U}{kT}\right) \quad (41)$$

where $\sigma_{nd.c.}$ is the nth-order d.c. conductivity ($n = 1, 3, 5, \ldots$), a is the hopping distance and P_0 is the probability of hopping as T approaches infinity. ΔU is the difference between the energies of the two states. If we take ratios, then

$$\frac{\sigma_{3d.c.}}{\sigma_{1d.c.}} = \frac{e^2 a^2}{24 k^2 T^2} \quad (42)$$

$$\frac{\sigma_{5d.c.}}{\sigma_{3d.c.}} = \frac{e^2 a^2}{80 k^2 T^2} \quad (43)$$

In much the same way as above, substituting $\sigma_{1d.c.}$, $\sigma_{3d.c.}$ and $\sigma_{5d.c.}$, obtained as best-fit parameters in linear and non-linear conductive spectra at each temperature, $a \simeq 100$–200 nm is obtained without any additional assumptions, and has no physical meaning in terms of the structure of a polyethylene oxide/salt complex [4–6, 24]. This indicates that $a \simeq 100$–200 nm is not as precise as $a^* \simeq 4$–5 nm obtained by the dynamic percolation model. Consequently, we find that the dynamic percolation model is superior to the two-site simple hopping model. As mentioned earlier, even with only the experimental values, we can determine whether the two-site hopping model or the dynamic percolation model is better without any additional assumptions. Thus, non-linear measurements have been extremely useful in determining the mechanism of ion transport in ion-conducting polymers.

5. Conclusion

A new experimental system has been developed which enables measurements of linear as well as nonlinear complex conductivities. Using this system, we measured the frequency dependence of linear to fifth-order non-linear complex conductivities in a polyethylene oxide/salt complex. We proposed a new empirical function to reproduce the observed linear and nonlinear conductive spectra which show the complicated characteristic frequency dependence together with the relaxation phenomenon. Furthermore, we found that the validity of the basic parameters can be examined without any additional assumptions by using the values of non-linear conductivities obtained from experiments. Using this method, we determined whether the two-site hopping model or the dynamic percolation model is better without any additional assumptions. We then evaluated the basic parameters, such as the hopping distance in the two-site hopping model or the size of a connected cluster of the effective sites capable of ion hopping in the dynamic percolation model, which characterize the behaviour of ion transport in ion-conducting polymers. As a result, we conclude that the dynamic percolation model is consistent with the prediction based on the structure of a polyethylene oxide/salt complex. Thus, the non-linear technique developed here appears to be useful for the empirical determination of the validity of the theory.

Acknowledgements

We thank Professor T. Furukawa, Science University of Tokyo, for useful comments, Dr Y. Ueno, Waseda University, for providing us with various ion-conducting polymers, and Dr M. Date, Institute of Physical and Chemical Research, for his support. We also thank T. Suzuki, a graduate of Waseda University Honjyo Senior High School, for his technical assistance.

References

1. D. E. FENTON, J. M. PARKER and P. V. WRIGHT, *Polymer* **14** (1973) 589.
2. P. V. WRIGHT, *Br. Polym. J.* **7** (1975) 319.
3. P. V. WRIGHT, *J. Polym. Sci.* **14** (1976) 955.
4. J. R. MacCALLUM and C. A. VINCENT (eds) "Polymer Electrolyte Reviews – 1" (Elsevier Applied Science, London, New York, 1987).
5. *Idem*, "Polymer Electrolyte Reviews – 2" (Elsevier Applied Science, London, New York, 1989).
6. D. F. SHRIVER and M. A. RATNER, *Chem. Rev.* **88** (1988) 109.
7. M. B. ARMAND, *Ann. Rev. Mater. Sci.* **16** (1986) 245.
8. M. WILLIAMS, R. F. LANDEL and J. D. FERRY, *J. Am. Chem. Soc.* **77** (1955) 3701.
9. H. VOGEL, *Phys.* **22** (1921) 645.
10. G. TAMMAN and W. Z. HESSE, *Anorg. Allg. Chem.* **156** (1926) 245.
11. G. S. FULCHER, *J. Am. Ceram. Soc.* **8** (1925) 339.
12. M. GOLDSTEIN, *J. Phys. Chem.* **77** (1973) 667.

13. G. ADAM and J. H. GIBBS, *J. Chem. Phys.* **43** (1965) 139.
14. C. A. ANGELL, *Solid State Ionics* **9/10** (1983) 3.
15. J. J. FONTANELLA, M. C. WINTERSGILL, M. K. SMITH, J. SEMANCIK and C. G. ANDEEN, *J. Appl. Phys.* **60** (1986) 2665.
16. T. WONG, M. BRODWIN, J. I. McOMBER and D. F. SHRIVER, *Solid State Commun.* **35** (1980) 591.
17. R. VAITKUS, A. KEZIONICS, A. SAUMLIONIS, A. ORLIUKAS and V. SKRITSKIJ, *Solid State Ionics* **40/41** (1990) 922.
18. K. FUNKE, *ibid.* **18/19** (1986) 183.
19. A. I. TIPTON, M. C. LONERGAN, M. A. RATNER, D. F. SHRIVER, T. Y. WONG and K. HAN, *J. Phys. Chem.* **98** (1994) 4148.
20. S. D. DRUGER, M. A. RATNER and A. NITZAN, *Phys. Rev.* **B31** (1985) 3939.
21. A. K. HARISON and R. ZWANZIG, *Phys. Rev.* **A32** (1985) 1072.
22. T. FURUKAWA, K. NAKAJIMA, T. KOIZUMI and M. DATE, *Jpn J. Appl. Phys.* **26** (1987) 1039.
23. O. NAKADA, *J. Phys. Soc. Jpn* **15** (1960) 2280.
24. J. PRZYLUSKI, K. SUCH, H. WYCISLIK, W. WIECZOREK and Z. FLORIANCZYK, *Synth. Metals* **35** (1990) 241.
25. Y. UENO, Y. TAJITSU and T. FURUKAWA, *Polymer* **33** (1992) 665.
26. J. F. JOHNSON and R. H. COLE, *J. Am. Chem Soc.* **73** (1951) 4356.
27. H. FROHLICH, "The Theory of Dielectrics", 2nd Edn (Clarendon, Oxford, 1958).
28. N. F. MOTT and E. A. DAVIS, "Electronic Processes in Non-Crystalline Materials", 2nd Edn (Clarendon, Oxford, 1979).

Received 15 February
and accepted 17 October 1995